Developmental Cell
Article

Kinesin-1 Prevents Capture of the Oocyte Meiotic Spindle by the Sperm Aster

Karen L.P. McNally,[1,2] Amy S. Fabritius,[1,2] Marina L. Ellefson,[1,2] Jonathan R. Flynn,[1,2] Jennifer A. Milan,[1,2] and Francis J. McNally[1,*]
[1]Department of Molecular and Cellular Biology, 149 Briggs Hall, University of California, Davis, Davis, CA 95616, USA
[2]These authors contributed equally to this work
*Correspondence: fjmcnally@ucdavis.edu
DOI 10.1016/j.devcel.2012.01.010

SUMMARY

Centrioles are lost during oogenesis and inherited from the sperm at fertilization. In the zygote, the centrioles recruit pericentriolar proteins from the egg to form a mature centrosome that nucleates a sperm aster. The sperm aster then captures the female pronucleus to join the maternal and paternal genomes. Because fertilization occurs before completion of female meiosis, some mechanism must prevent capture of the meiotic spindle by the sperm aster. Here we show that in wild-type *Caenorhabditis elegans* zygotes, maternal pericentriolar proteins are not recruited to the sperm centrioles until after completion of meiosis. Depletion of kinesin-1 heavy chain or its binding partner resulted in premature centrosome maturation during meiosis and growth of a sperm aster that could capture the oocyte meiotic spindle. Kinesin prevents recruitment of pericentriolar proteins by coating the sperm DNA and centrioles and thus prevents triploidy by a non-motor mechanism.

INTRODUCTION

Centrioles play essential roles in controlling the number of spindle poles during mitosis and in assembly of cillia and are thus subject to strict number control (Leidel and Gönczy, 2005). In *Caenorhabditis elegans*, centrioles are eliminated early during oogenesis and reintroduced by sperm during fertilization. This model is supported by electron microscopy showing an absence of centrioles at the poles of oocyte meiotic spindles (Albertson and Thomson, 1993) and the presence of centrioles in mature sperm (Ward et al., 1981) and at the male pronucleus of the zygote (Pelletier et al., 2006). In addition, GFP fusions to centriolar and pericentriolar proteins label distinct foci associated with nuclei in the distal gonad (early oogenesis), no foci in the proximal gonad (later oocytes) (Zhou et al., 2009), then again label discrete foci in fertilized zygotes (Pelletier et al., 2006). Failure to eliminate maternal centrioles has been reported to result in multipolar mitotic spindles in the *C. elegans* zygote (Kim and Roy, 2006) and fertilization by more than one sperm results in multipolar mitotic spindles in several species (Harris et al., 1980; Navara et al., 1994).

Sperm-derived centrioles recruit centriolar (Pelletier et al., 2006) and pericentriolar (Hamill et al., 2002) proteins from the egg cytoplasm to form a mature centrosome that nucleates a sperm aster. Recruitment of maternal pericentriolar proteins to sperm centrioles has been reconstituted in *Xenopus* egg extracts and occurs in as little as 7 min (Stearns and Kirschner, 1994). The radial array of microtubules that constitutes the sperm aster captures the female pronucleus after meiosis to bring maternal and paternal chromosomes into close proximity before formation of the first mitotic spindle (Oegema and Hyman, 2006). The fact that fertilization occurs during female meiosis in most animal species (prometaphase I in *C. elegans*) necessitates mechanisms to prevent interference with the female meiotic spindle by the sperm aster. Little is known about these mechanisms.

Earlier studies have shown that in *Urechis* (Gould and Stephano, 1999) and *Crassostrea* (Stephano and Gould, 2000), sperm aster formation is completely suppressed until after completion of meiosis. In contrast, the size of the sperm aster is limited during meiosis in starfish zygotes (Stephano and Gould, 2000). In *Spisula*, maternal and paternal centrioles share the same cytoplasm during female meiosis; however, the ability of the paternal centrioles to form a sperm aster is suppressed during meiotic metaphase I when maternal centrioles drive assembly of two microtubule asters utilized in meiotic chromosome segregation (Wu and Palazzo, 1999). Wu and Palazzo suggested that failure to suppress the sperm aster during metaphase I might result in chromosome misegregation by a tripolar meiotic spindle. The mechanism that prevents sperm aster formation during metaphase I in *Spisula* has not been addressed and the timing of sperm aster formation during female meiosis has not been addressed in most species.

In this study, we demonstrate that recruitment of maternal pericentriolar proteins to sperm-derived centrioles is completely suppressed from prometaphase I through anaphase II in *C. elegans* zygotes. We show that this suppression is mediated by kinesin-1 and a kinesin-binding protein and that these proteins form a shell surrounding the sperm DNA/centriole complex in the zygote. We also demonstrate that premature sperm asters can capture female meiotic spindles and prevent polar body extrusion.

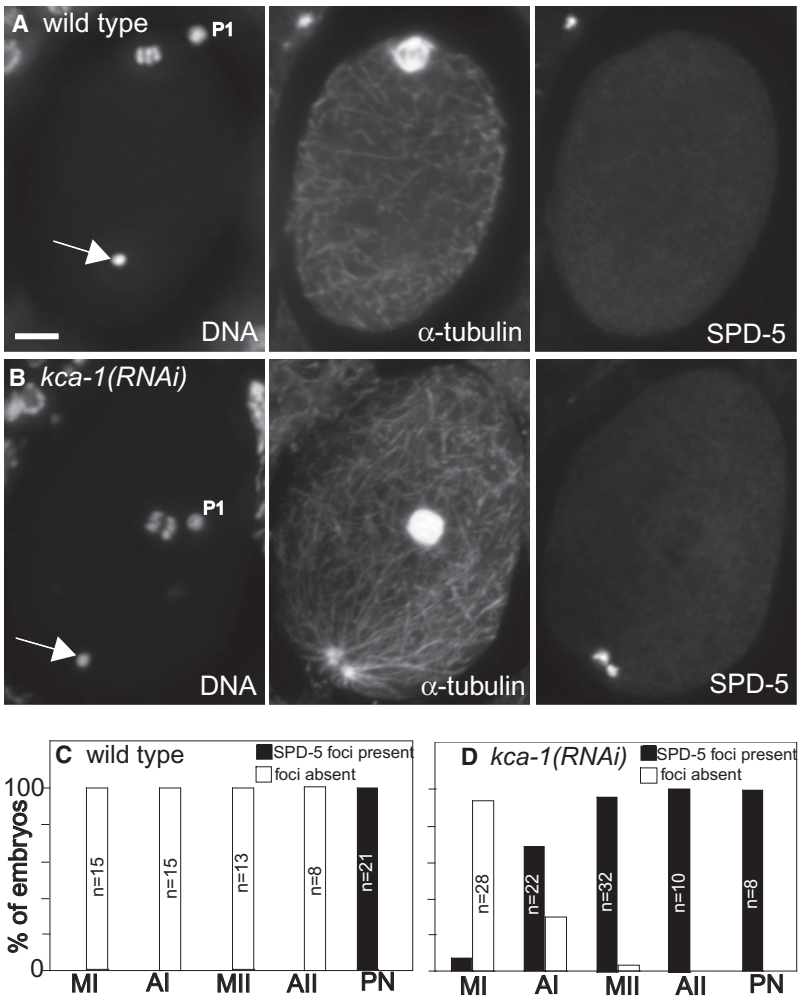

Figure 1. SPD-5 Accumulates on Centrosomes Prematurely in Embryos Depleted of the Kinesin-1 Regulator, KCA-1

Maximum intensity projections of 3D image stacks of fixed meiotic embryos stained with DAPI (DNA), anti-α tubulin antibody, and anti-SPD-5 antibody.

(A) Wild-type metaphase II embryo has no microtubule asters or SPD-5 associated with the sperm DNA. Sperm DNA indicated by arrow. P1, first polar body.

(B) *kca-1(RNAi)* anaphase II embryo has two microtubule asters and two foci of SPD-5 associated with the sperm DNA.

(C and D) Quantification of the percentage of embryos exhibiting premature centrosome maturation at different stages of meiosis.

MI, metaphase I; AI, anaphase I; MII, metaphase II; AII, anaphase II; PN, pronuclear stage. Scale bar represents 5 μm. See also Table S1 and Figure S1.

RESULTS

Depletion of Kinesin-1 Heavy Chain or the Kinesin-Binding Protein, KCA-1, Causes Premature Centrosome Maturation and Sperm Aster Assembly during Oocyte Meiosis

In wild-type *C. elegans* zygotes, the pericentriolar proteins SPD-5 and γ-tubulin are not recruited to the sperm centrioles until after the second polar body has been extruded and the male pronucleus has formed and moved to the cortex (see Figure S1 and Table S1 available online). Thus, some mechanism must prevent recruitment of SPD-5 and γ-tubulin to the sperm-derived centrioles from the time of fertilization at prometaphase I through completion of meiosis II, a period lasting 35 min (McNally and McNally, 2005). In striking contrast, both SPD-5 and γ-tubulin are recruited to the sperm centrioles as early as anaphase I after depletion of the kinesin-1 heavy chain, UNC-116, or the kinesin cargo adaptor, KCA-1 (Figure 1; Table S1). In addition, sperm asters consisting of long microtubules grew from the premature centrosomes in *kca-1(RNAi)* meiotic embryos (Figure 1) but not in wild-type meiotic embryos. The GFP::γ-tubulin recruited to sperm centrosomes in *kca-1(RNAi)* embryos (Table S1) was expressed in oocytes but not in sperm before fertilization. Identical results were obtained with GFP::TAC-1 that was expressed in oocytes but not in sperm (data not shown). Thus, the premature centrosome maturation observed involves recruitment of maternal pericentriolar proteins to the sperm centrioles. Because worms were exposed to RNAi treatment at the L4 stage when spermatogenesis is already complete, premature centrosome maturation must be caused by depletion of UNC-116 or KCA-1 from the egg cytoplasm rather than defects in spermatogenesis. Consistent with this interpretation, we previously showed that fertilization by wild-type sperm does not decrease the embryonic lethality of *unc-116(RNAi)* or *kca-1(RNAi)* (Yang et al., 2005).

In an attempt to expand the list of gene products involved in suppression of sperm centrosome maturation, we examined a number of candidate proteins. The breast cancer associated ubiquitin ligase BRCA-1/BRD-1 inhibits centrosome maturation in mitotic mammalian cells (Parvin, 2009) but loss-of-function mutations in these genes did not cause premature centrosome maturation during *C. elegans* meiosis (Table S1). The conserved protein, SZY-20, suppresses sperm centrosome maturation in *C. elegans* mitotic embryos (Song et al., 2008) but a *szy-20(ts)* mutant did not cause premature centrosome maturation during meiosis (Table S1). MAP kinase has been implicated in suppression of sperm aster formation during meiosis in marine invertebrates (Gould and Stephano, 1999; Stephano and Gould, 2000). However, we observed no SPD-5 staining at the sperm centrioles in meiotic embryos dissected from *mpk-1(ga111ts)* (Lee et al., 2007) worms after a 24 hr shift to nonpermissive temperature (Table S1). KCA-1 was reported to interact with the heterochromatin protein, HPL-2 (Li et al., 2004), which binds to nucleosomes containing trimethyl K9 histone H3. Although the sperm DNA stained with an anti-trimethyl K9 H3 antibody in 20/20 meiotic embryos, we did not observe premature centrosome maturation in *hpl-2(tm1489)* (Schott et al., 2006) worms (Table S1). A loss-of-function mutation in *unc-14* (Table S1), a *Caenorhabditis*-specific regulator of kinesin-1 in the nervous system (Sakamoto

et al., 2005), did not result in SPD-5 accumulation at sperm centrioles. Loss-of-function mutations in the conserved kinesin-1 regulators UNC-16 (Sakamoto et al., 2005), UNC-76 (Toda et al., 2008), or UNC-33 (Tsuboi et al., 2005) caused accumulation of a very small focus of SPD-5 in a small fraction of meiotic embryos but these were never associated with a microtubule aster (Table S1). These results support a specific role for kinesin-1 heavy chain and KCA-1 in suppression of sperm centrosome maturation.

Kinesin-1 Heavy Chain, Light Chain, and KCA-1 Form a Shell around the Sperm DNA and Centrioles during Meiosis

To test whether a complex of kinesin-1 and KCA-1 might act directly at the sperm centrioles during female meiosis, we carefully examined the localization of the kinesin-1 heavy chain, UNC-116, the kinesin-1 light chain, KLC-1, and KCA-1 in meiotic embryos. Anti-KCA-1 antibody labeled an irregular ring (average maximal diameter 5.18 ± 0.17 μm, n = 22) surrounding the sperm DNA (Figures 2B and 2D). This ring was absent from *kca-1(RNAi)* meiotic embryos (Figure S2E; Figure 2Q) and an irregular ring of similar diameter (5.8 ± 0.33 μm, n = 5) was labeled in living mCherry::KCA-1 meiotic embryos in utero (Figure 2E). Yolk granules are transported away from the cortex and packed in a central mass in meiotic embryos (McNally et al., 2010). In most meiotic embryos, the sperm DNA was outside the zone of centrally packed yolk granules (Figure S2F). In those embryos where the sperm DNA was within the packed mass of yolk granules, yolk granules were excluded from an irregular zone around the sperm DNA (Figures 2C and 2P) with an average maximal diameter (5.24 ± 0.19 μm, n = 20) similar to that of the KCA-1 ring. Antibodies specific for the kinesin-1 heavy chain, UNC-116, labeled a similar ring around the sperm DNA (Figures 2H and 2I) with a diameter (4.52 ± 0.12 μm, n = 20) slightly smaller than that of KCA-1. No anti-UNC-116 staining around the sperm DNA was observed in *unc-116(RNAi)* embryos (Figure 2Q; Figure S2D). Antibodies specific for the kinesin-1 light chain, KLC-1, also labeled a ring surrounding the sperm DNA in meiotic embryos (Figures 2K and 2M). This labeling was absent in *klc-1(RNAi)* meiotic embryos (Figure 2Q) and an identical ring was observed in living mCherry::KLC-1 meiotic embryos in utero (Figure 2L). The KLC-1 ring had a slightly smaller diameter than the KCA-1 ring (anti-KLC-1: 4.06 ± 0.12 μm, n = 14; mCherry::KLC-1: 4.63 ± 0.15 μm, n = 7). The rings of UNC-116, KLC-1, and KCA-1 around the sperm DNA in meiotic embryos were reminiscent of SPD-2, which is found in a ring around the DNA of mature sperm before fertilization and in the centrioles of mature sperm (Pelletier et al., 2004). SPD-2 antibodies labeled a much smaller ring around the sperm DNA in meiotic embryos (2.20 ± 0.05 μm, n = 12) and the centrioles (Figure 2O). Because identical SPD-2 localization has been previously reported in mature sperm (Pelletier et al., 2004), we infer that the SPD-2 in this ring is paternally derived.

The smaller diameter of the SPD-2 around the sperm DNA suggested that paternal SPD-2 might be required to recruit maternal KCA-1 to the sperm DNA and centrioles. Because SPD-2 is required for spermatogenesis and RNAi is not effective on mature sperm, we utilized a fast-acting ts allele of *spd-2* (O'Rourke et al., 2011) to inactivate SPD-2 just before fertilization. Anti-KCA-1 staining of meiotic embryos dissected from *spd-2(or293)* worms raised at the permissive temperature of 16°C revealed rings of KCA-1 around the sperm DNA identical to those seen in wild-type. When *spd-2(ts)* worms were shifted to the nonpermissive temperature of 25°C for 6 hr, the intensity of anti-KCA-1 staining around the sperm DNA decreased. The enrichment of KCA-1 around the sperm DNA was quantified as the ratio of fluorescence intensity adjacent to the sperm DNA divided by the fluorescence intensity of the adjacent cytoplasm and expressed as percent. At permissive temperature, KCA-1 was enriched around the sperm DNA by 209.9 ± 9.6% (n = 24) or 2-fold relative to the adjacent cytoplasm. At nonpermissive temperature this enrichment was reduced to 139.5 ± 5.2% (n = 30) or 1.4-fold. The results of Student's t test indicated that these numbers are significantly different ($p < 0.0001$) indicating that SPD-2 is required to recruit KCA-1 to the sperm DNA and centrioles. SPD-2 is likely only partially inactivated by this ts allele as SPD-2 antibody staining at the sperm DNA and centrioles of meiotic embryos appeared wild-type; thus, only partial reduction in the KCA-1 ring would be expected. Our results are consistent with a model in which KCA-1 and kinesin-1 are recruited to the sperm DNA and centrioles by paternal SPD-2. SPD-2 is required for recruitment of SPD-5 and γ-tubulin to centrioles (Pelletier et al., 2004; Kemp et al., 2004), therefore we propose that kinesin-1 and KCA-1 are components of a structure that might prevent interaction between maternal SPD-5 and paternal SPD-2 and thus prevent centrosome maturation.

Kinesin-1/KCA-1 Positions the Sperm DNA/Centriole Complex within the Meiotic Embryo by a Mechanism Distinct from the Suppression of Centrosome Maturation

In addition to premature centrosome maturation, the position of the sperm DNA/centriole complex during meiosis was dramatically different in *kca-1(RNAi)* embryos than in wild-type embryos. In wild-type meiotic embryos, the sperm DNA was found deep in the cytoplasm, usually in the future posterior quadrant of the embryo from metaphase I through anaphase II (Figures 1A, 2A–2C, and 3A; Figures S1A, S1B, and S1I). The male pronucleus moved into close proximity to the future posterior cortex around the time of centrosome maturation (Figures S1F and S1I, 22 min) as previously reported (Rappleye et al., 2002). In contrast, the sperm DNA was observed in close contact with the future posterior cortex at all stages of meiosis in fixed *kca-1(RNAi)* embryos (Figures 1B and 3A). One interpretation of these results is that in wild-type embryos, the sperm DNA/centriole complex is transported inward from the site of fertilization in a KCA-1-dependent manner and that the sperm DNA/centriole complex moves back to the cortex after meiosis. In this scenario, the sperm DNA remains at the site of fertilization in *kca-1(RNAi)* embryos. Alternatively, the sperm DNA might move inward from the site of fertilization in a KCA-1-independent manner but move back to the cortex prematurely in *kca-1(RNAi)* embryos, possibly due to premature sperm aster formation.

If the sperm DNA moved inward normally in *kca-1(RNAi)* embryos but moved back to the cortex prematurely, then the sperm DNA would be expected to be further from the cortex early in meiosis than late in meiosis. The data in Figure 3A, however, indicate that the distance of the sperm DNA from the

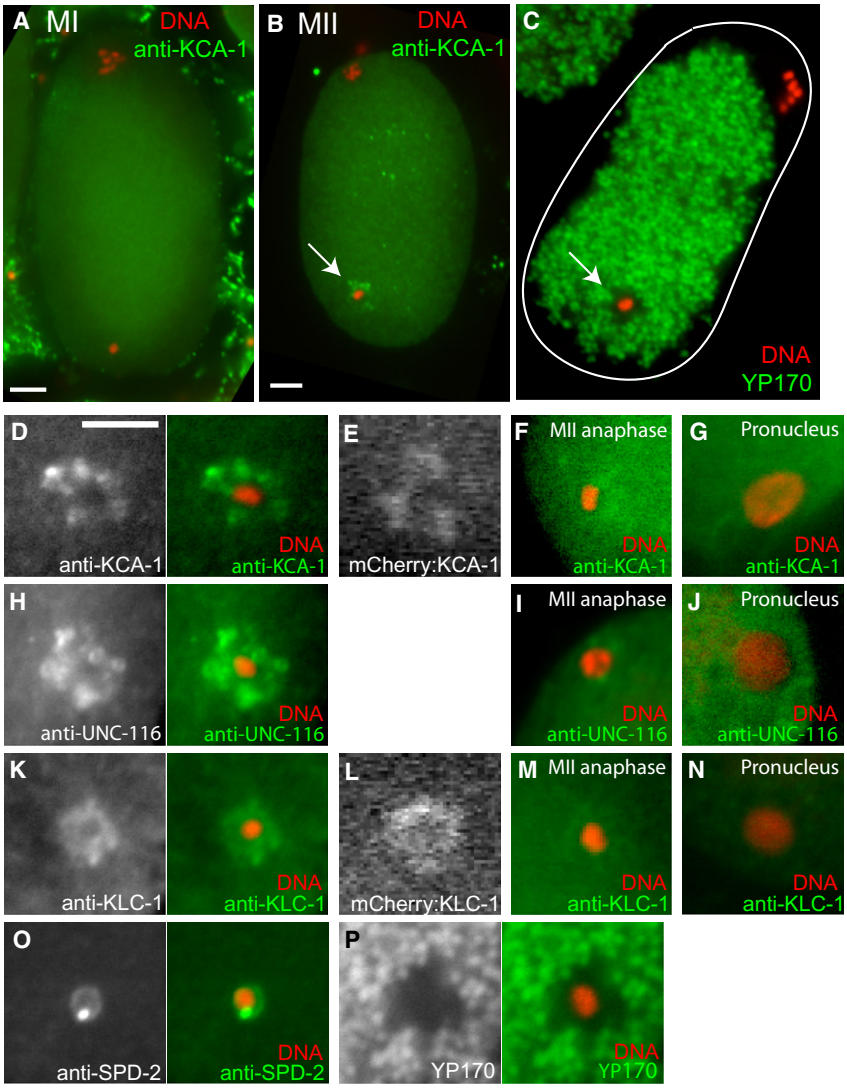

Q Relative staining intensity around the sperm DNA (percent of cytoplasmic staining intensity).

antibody	early MI meta	late MI meta	MI anaphase	MII metaphase	MII anaphase
KCA-1:	101** +/- 1.7 n=7	121 +/- 4.5 n=15	146 +/- 10 n=6	153 +/- 9.8 n=10	112 +/- 4.5 n=9
KLC-1:		129 +/- 4.4 n=10	123 +/- 4.9 n=5	140 +/- 7.1 n=12	108 +/- 2.4 n=7
UNC-116:	108** +/- 3.7 n= 9	145 +/- 10 n=12	141 +/- 8.9 n=7	139 +/- 5.3 n=9	122 +/- 4.9 n=7

antibody	Pronuclear stage	all stages	
KCA-1:	102** +/- 4.7 n=9	*kca-1(RNAi)*	99.0* +/- 1.9 n=18
KLC-1:	99.0* +/- 2.5 n=10	*klc-1(RNAi)*	99.8* +/- 0.5 n=17
UNC-116:	99.4* +/- 4.1 n=10	*unc-116(RNAi)*	99.9* +/- 1.7 n=28

Figure 2. KCA-1, KLC-1, and UNC-116 Are Concentrated in a Yolk-Free Zone Surrounding the Sperm DNA in Meiotic Embryos

(A) In 7/8 metaphase I embryos, KCA-1 was packed in the central cytoplasm as previously reported (McNally et al., 2010).

(B) Metaphase II embryo with KCA-1 surrounding the sperm DNA (arrow). 20/22 embryos from anaphase I through anaphase II had KCA-1 staining around the sperm DNA.

(C) Fixed metaphase II embryo expressing tdimer2:YP170, a yolk granule marker, showing a yolk-free zone surrounding the sperm DNA (arrow).

(D) Enlarged view of anti-KCA-1 staining around the sperm DNA during metaphase II.

(E) Enlarged view of mCherry:KCA-1 around the sperm DNA in a living embryo in utero.

(F) The concentration of KCA-1 around the sperm DNA is reduced during anaphase II.

(G) No KCA-1 enrichment is apparent around the male pronucleus.

(H) Enlarged view of anti-UNC-116 staining around the sperm DNA in a metaphase II embryo.

(I) UNC-116 staining around the sperm DNA of an anaphase II embryo.

(J) No UNC-116 staining is apparent around the male pronucleus.

(K) Anti-KLC-1 staining around the sperm DNA of a metaphase II embryo.

(L) mCherry:KLC-1 around the sperm DNA in a living meiotic embryo in utero. The time since ovulation for this embryo would suggest metaphase II.

(M) Anti-KLC-1 staining around the sperm DNA of an anaphase II embryo.

(N) No anti-KLC-1 staining is apparent around the male pronucleus.

(O) Anti-SPD-2 staining of the sperm centrioles and a ring around the sperm DNA in a metaphase II embryo.

(P) Enlarged view of the yolk-free zone around the sperm DNA in a fixed metaphase II embryo.

(Q) Staining intensity around the sperm DNA was divided by the staining intensity of the adjacent cytoplasm, multiplied by 100 and expressed as percentages.

± indicates standard error of the mean. Asterisks indicate that the number is significantly different than the pooled values for wild-type metaphase I through anaphase II using Student's t test (*$p < 0.01$, **$p < 0.05$). Early metaphase I: sperm DNA <3 μm from cortex). Late metaphase I: sperm DNA >3 μm from cortex. Scale bars represent 5 μm. Magnification is the same in (A)–(C) and (D)–(P). See also Figure S2.

cortex does not vary between metaphase I and metaphase II. If premature centrosome maturation caused premature return of the internalized sperm to the cortex, then sperm DNA with SPD-5-positive centrosomes should be close to the cortex while sperm DNA without SPD-5-positive centrosomes in *kca-1(RNAi)* embryos should be as far from the cortex as in wild-type embryos. As shown in Figure 3B, sperm DNA without SPD-5-positive centrosomes was still much closer to the cortex than in wild-type. Sperm DNA with SPD-5-positive centrosomes was closer to the cortex than SPD-5-negative sperm DNA in *kca-1(RNAi)* embryos (Figure 3B), possibly indicating that sperm asters can stabilize the position of the sperm DNA at the cortex. In addition, *kca-1(RNAi)* decreased the distance between sperm and cortex in *spd-2(ts)* embryos which should be defective in centrosome maturation and aster formation (Figure 3B). These data support a model in which the sperm DNA/centriole complex

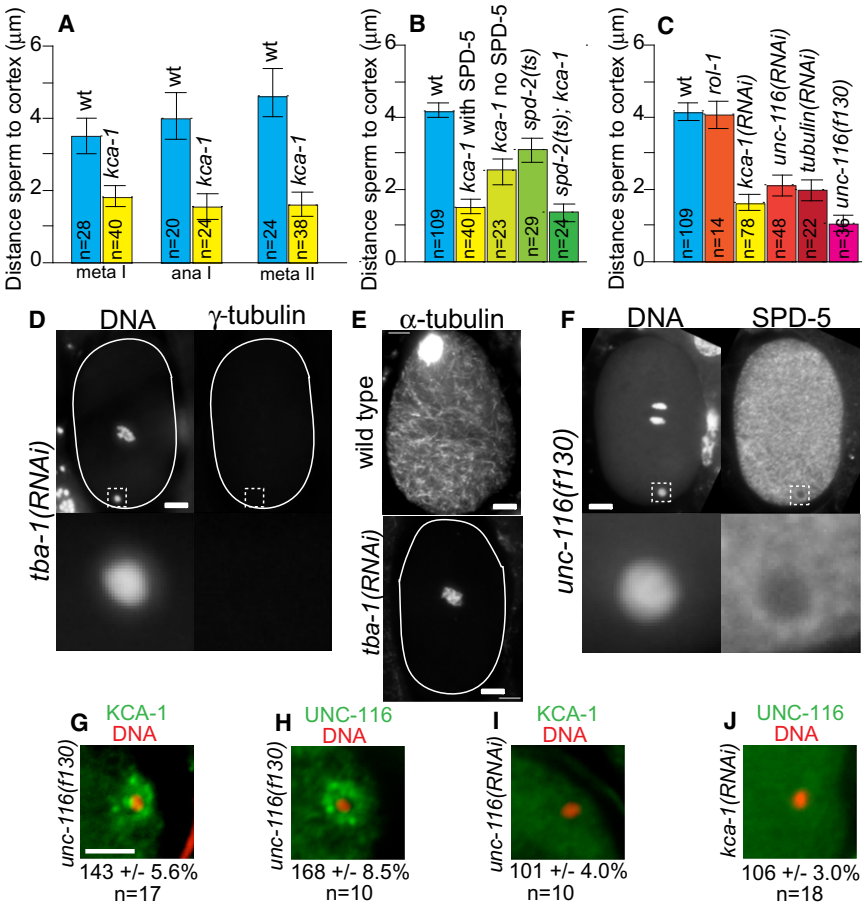

Figure 3. Microtubules Are Not Required for Suppression of Sperm Centrosome Maturation

(A–C) Average distances of the sperm DNA from the nearest point on the cortex determined from fixed meiotic embryos. (A) Comparison of sperm distance from the cortex in wild-type versus *kca-1(RNAi)* embryos at metaphase I (meta I), anaphase I (ana I) and metaphase II (meta II). B. Average distance of sperm DNA from the cortex in mixed stage meiotic embryos (metaphase I through anaphase II) in wild-type, *kca-1(RNAi)* embryos with SPD-5 foci at the sperm DNA and *kca-1(RNAi)* embryos without SPD-5 foci at the sperm. *spd-2(ts)* indicates *spd-2(or293)* grown at nonpermissive temperature for 6 hr and *spd-2(ts); kca-1* indicates *spd-2(or293); kca-1(RNAi)* grown at nonpermissive temperature for 6 hr. (C) Average distance of sperm DNA from the cortex in mixed stage meiotic embryos (metaphase I through anaphase II) of the indicated genotype. *rol-1* is a body wall collagen mutant that renders worms more sensitive to *unc-116(RNAi)*. Thus, the *unc-116(RNAi)* worms were actually *rol-1; unc-116(RNAi)*. *tubulin(RNAi)* indicates *tba-1(RNAi)*. Error bars in (A)–(C) indicate standard error of the mean.

(D and E) Fixed immunofluorescence images of meiotic embryos from worms depleted of α-tubulin (TBA-1). (D) 0/12 *tba-1(RNAi)* meiotic embryos had maternal GFP: γ-tubulin foci associated with the sperm DNA. (E) Anti-α-tubulin immunofluorescence reveals that *tba-1(RNAi)* meiotic embryos completely lack cytoplasmic microtubules.

(F) Anti-SPD-5 immunofluorescence revealed that no SPD-5 was recruited to centrioles in 7/7 *unc-116(f130)* meiotic embryos. No anti-γ-tubulin staining foci were associated with 30/30 *unc-116(f130)* meiotic embryos (data not shown). Nearly all meiotic anaphase spindles were in the center of the *unc-116(f130)* embryo.

(G–J) Both KCA-1 (G) and UNC-116 (H) were concentrated in a ring around the sperm DNA of *unc-116(f130)* meiotic embryos whereas neither protein was concentrated around the sperm DNA in *unc-116(RNAi)* meiotic embryos (I) or in *kca-1(RNAi)* meiotic embryos (J). Ratio indicates the fluorescence intensity of staining around the sperm DNA divided by the fluorescence intensity of the adjacent cytoplasm expressed as percentages. n, the number of embryos used to obtain the average ratio shown.

± indicates standard error of the mean. Scale bar represents 5 µm. See also Figure S3.

moves inward from the site of fertilization by a KCA-1-dependent mechanism.

We previously presented evidence that yolk granules are transported inward, away from the cortex by kinesin-1/KCA-1 on cytoplasmic microtubules that extend diagonally inward from the cortex (McNally et al., 2010). If the sperm DNA/centriole complex were also transported inward as direct cargo of kinesin-1/KCA-1, this transport should be blocked when kinesin-1 heavy chain, UNC-116, is depleted or when cytoplasmic microtubules are depleted by *tubulin* (RNAi). Indeed, the sperm DNA remained close to the cortex in *unc-116(RNAi)*, *tubulin (RNAi)* or *unc-116(f130)* meiotic embryos (Figure 3C). We also found that very early in wild-type meiosis, sperm DNA without kinesin-1 or KCA-1 were closer to the cortex than sperm DNA with a kinesin-1/KCA-1 shell (Figure 2Q). This suggests that a shell of maternal kinesin-1/KCA-1 must assemble around the sperm DNA/centriole complex before it is transported inward on microtubules.

Premature centrosome maturation did not occur in *tubulin(RNAi)* or *unc-116(f130)* meiotic embryos (Figures 3D and 3F; Figure S3A). Cytoplasmic microtubules were absent or greatly reduced in *tubulin(RNAi)* meiotic embryos (Figure 3E) and maternal chromosomes were in a mass in the center of the meiotic embryo as previously reported (Yang et al., 2003), presumably because both kinesin-dependent (Yang et al., 2005) and dynein-dependent (Ellefson and McNally, 2009, 2011) meiotic spindle positioning mechanisms require cytoplasmic microtubules. Importantly, *tubulin(RNAi)* did not prevent centrosome maturation in postmeiotic embryos (Figure S3). Thus, kinesin-dependent suppression of centrosome maturation does not appear to require kinesin-dependent transport on microtubules. The *unc-116(f130)* mutant, which has a single amino acid substitution in kinesin heavy chain, causes a severe meiotic spindle positioning defect (Figure 3F) indicating that it lacks transport function. Thus, the ability of *unc-116(f130)* meiotic embryos to suppress centrosome maturation during meiosis (Figure 3F) further supports the hypothesis that microtubule-based transport is not required for suppression of centrosome maturation during meiosis. The findings that the sperm DNA is closely opposed to the plasma membrane in

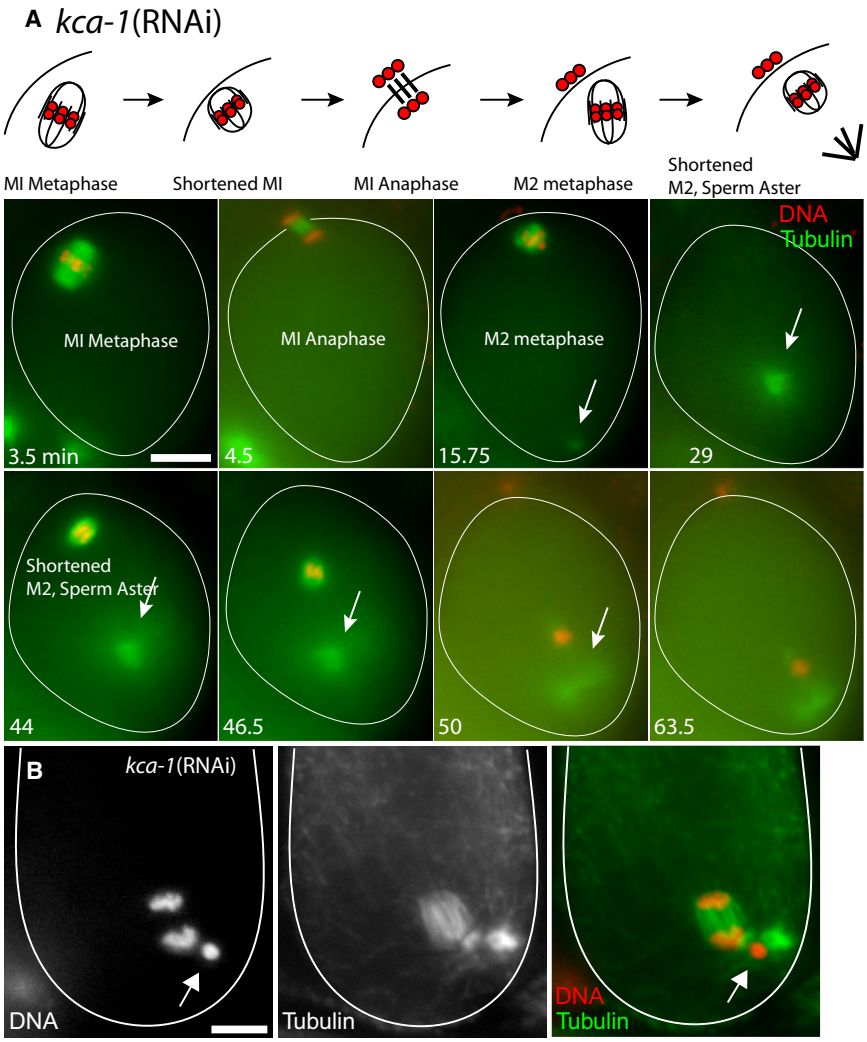

Figure 4. Sperm Asters Can Capture Female Meiotic Spindles

(A) Time-lapse sequence of an mCherry:histone, GFP:tubulin, *kca-1(RNAi)* embryo filmed in utero. The Metaphase I spindle, which is illustrated above the images and observed at 3.5 min, is at the future anterior end of the embryo. After the spindle shortens and rotates, the chromosomes separate during MI anaphase (4.5 min). The MII spindle then forms and is observed at a crosswise angle at 15.75 min. Also seen at this time-point is a small sperm aster at the future posterior end of the embryo (arrow). At 29 min the sperm aster has separated from the cortex and moved inward. The meiotic spindle is in a different focal plane at this time point. At 44–46.5 min, the shortened MII spindle is observed moving toward the sperm aster, which may have duplicated. At 50–63.5 min, the spindle and aster(s) move toward the posterior cortex. During this latter stage, the MII spindle has been reduced in size to that of an anaphase spindle. By 63.5 min, the MII spindle has traversed the entire length of the embryo. Scale bar represents 10 μm.

(B) Fixed *kca-1(RNAi)* embryo in which the sperm aster has captured an anaphase meiotic spindle. Arrow indicates sperm DNA. Scale bar represents 10 μm.

unc-116(f130) embryos and *tubulin(RNAi)* embryos (Figure 3C) but centrosomes fail to mature, rule out the possibilities that premature centrosome maturation is caused by cortical contact of the sperm centrioles or that inward transport of the sperm centrioles suppresses maturation. Both UNC-116 (Figure 3H) and KCA-1 (Figure 3G) were still present in a ring around the sperm DNA during meiosis in *unc-116(f130)* embryos but not in *unc-116(RNAi)* embryos (Figure 3I). These results further support a model in which the ring of kinesin-1/KCA-1 surrounding the sperm DNA/centriole complex directly inhibits recruitment of pericentriolar proteins to the sperm centrioles.

Premature Sperm Asters Capture the Oocyte Meiosis II Spindle

To test whether the sperm asters that form in *kca-1(RNAi)* meiotic embryos are capable of capturing the female meiotic spindle, we monitored microtubules and chromosomes by time-lapse imaging in GFP:tubulin, mCherry:histone, *kca-1(RNAi)* meiotic embryos in utero. In 6/24 time-lapse sequences, the sperm asters captured the meiosis II spindle (Figure 4A). Following three of the six spindle-capture events, three pronuclei (rather than two) were detected in the embryos by DIC microscopy. The other three examples of spindle capture resulted in arrested embryos. This result indicates that capture of the meiosis II spindle by a premature sperm aster can lead to triploidy by preventing extrusion of the second polar body.

We hypothesized that the low frequency of spindle capture in time-lapse sequences of *kca-1(RNAi)* embryos might be because the sperm derived centrosomes are too far away from the meiotic spindle in the majority of embryos. In all six examples of spindle capture, the sperm asters were initially stationary at the future posterior cortex, consistent with sperm position in fixed *kca-1(RNAi)* embryos (Figure 3). In each example of spindle capture, the meiosis II spindle initiated directed migration toward the sperm asters only after the sperm asters moved inward to within an average distance of 15.7 ± 0.8 μm (n = 5) of the spindle. In *kca-1(RNAi)* time-lapse sequences where spindle capture did not occur, the sperm aster remained close to the future posterior cortex and the closest distance between spindle and sperm aster was 23.5 ± 2.0 μm (n = 14). These results suggest that spindle capture is rare in *kca-1(RNAi)* embryos because the sperm aster is stationary at the future posterior end of the embryo where it is beyond a threshold capture distance of 17 μm. All six spindle capture events occurred at times indicating that the cell cycle was being delayed by photodamage relative to previous measurements of cell-cycle timing in *kca-1(RNAi)* and wild-type embryos (Yang et al., 2005). If photodamage-induced cell-cycle delay causes dissociation of the sperm aster from the future posterior cortex,

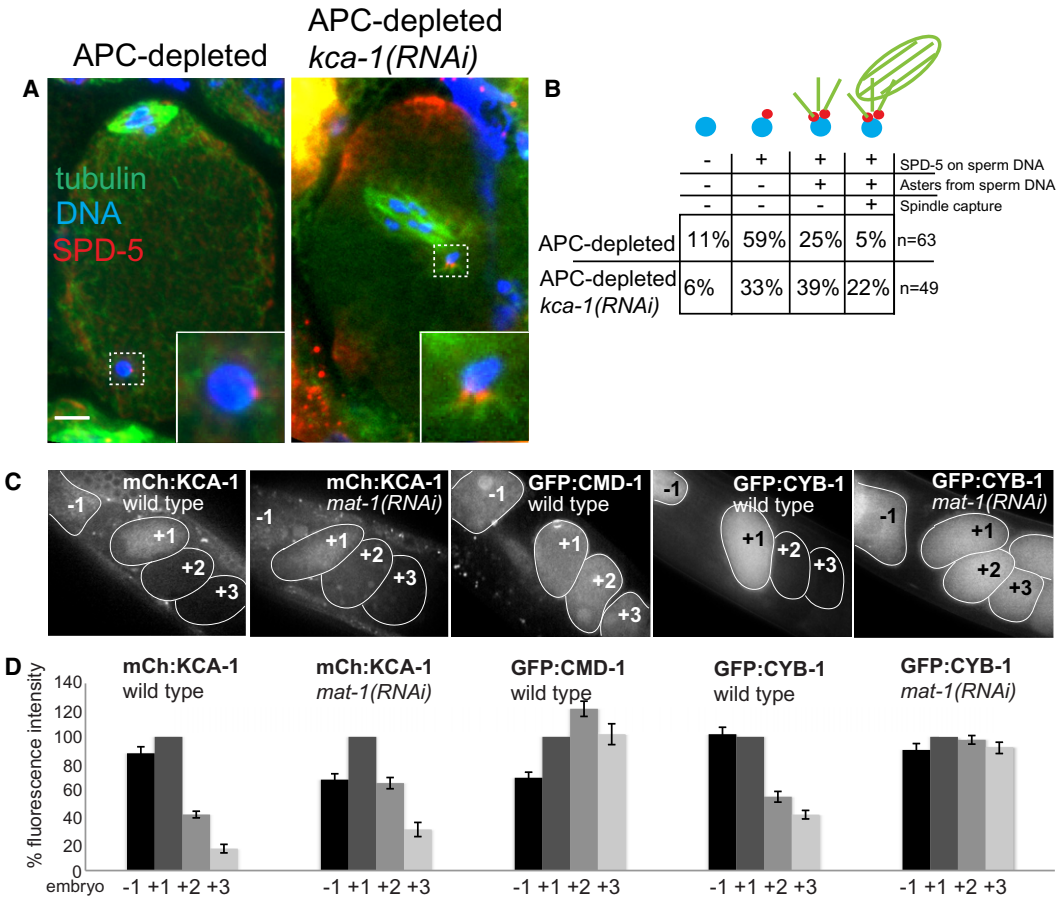

Figure 5. KCA-1 Is Degraded after Meiosis

(A) *mat2(ts);* GFP:tubulin and *mat2(ts);kca-1(RNAi)*; GFP:tubulin worms, which accumulate metaphase-I-arrested embryos in the uterus were fixed and stained with DAPI and SPD-5. Insets show blowup images of the sperm DNA.

(B) Embryos were scored for the presence of a SPD-5 focus at the sperm nucleus, GFP:tubulin-positive sperm aster and for spindle capture by the sperm aster. Scale bar represents 5 μm.

(C) Living worms expressing mCherry:KCA-1, GFP:calmodulin or GFP:CYB-1 were anesthetized and imaged by spinning disk confocal microscopy.

(D) For each worm, the fluorescence intensity of the +1 embryo was defined as 100% and the relative fluorescence intensity of the +2 and +3 embryos was determined and averaged over multiple worms. The fluorescence intensity of mCherry:KCA-1 decreased in +2 and +3 embryos of wild-type worms (n = 11) indicating proteolysis. No such proteolysis of calmodulin was observed (n = 11) and proteolysis of KCA-1 still occurred in metaphase I-arrested, *mat-1(RNAi)* embryos (n = 12). In contrast, proteolysis of cyclin B1 occurred in wild-type worms (n = 12) but was completely blocked in *mat-1(RNAi)* embryos (n = 12). Error bars indicate standard error of the mean. Scale bar represents 15 μm.

then spindle capture events should be rare among fixed *kca-1(RNAi)* embryos. As expected, only one spindle capture event was observed among 42 fixed *kca-1(RNAi)* embryos (Figure 4B).

To further test the hypothesis that spindle capture was promoted by a prolonged time in meiosis, we monitored meiotic spindles in embryos arrested in metaphase I by depletion of an anaphase promoting complex subunit with a *mat-2(ts)* mutant. We analyzed fixed metaphase I embryos from *mat-2(ts);kca-1(RNAi)* worms that correspond to an arrest period of 0–92 min (see Experimental Procedures). As shown in Figures 5A and 5B, spindle capture events occurred in 22% of metaphase-arrested, *kca-1(RNAi)* embryos. This result confirms that a delay in meiosis allows time for spindle capture, possibly because the sperm aster dissociates from the posterior cortex after an extended period in meiosis.

SPD-5 was also recruited to sperm centrioles in the majority of *mat-2(ts)*, metaphase-arrested embryos that were otherwise wild-type (Figures 5A and 5B). The majority of SPD-5-positive sperm centrosomes in *mat-2(ts)* embryos did not have an associated sperm aster, indicating a partial derepression of sperm centrosome maturation. In two time-lapse sequences of GFP:tubulin in metaphase-arrested *mat-2(ts)* embryos filmed in utero, sperm asters formed at 25 and 30 min after ovulation. These times are close to the times that wild-type meiotic embryos would complete meiosis and mature their centrosomes. These observations led to the hypothesis that KCA-1 might be degraded at the end of meiosis in wild-type embryos and that this degradation might still occur in APC-depleted embryos.

Postmeiotic Centrosome Maturation Is Initiated by Degradation of KCA-1 during Meiosis

To test whether degradation of KCA-1 occurs at the end of meiosis to allow wild-type centrosome maturation, we captured spinning disk confocal images of mCherry:KCA-1 in living

embryos in utero (Figure 5C). Embryos in the +1 position (adjacent to the spermatheca) revealed KCA-1 packed in the central cytoplasm. This pattern matched that observed in fixed metaphase I embryos by anti-KCA-1 immunofluorescence (Figure 2A; McNally et al., 2010). The cytoplasmic fluorescence intensity of mCherry:KCA-1 dropped in the +2 and +3 embryos (Figures 5C and 5D) suggesting proteolysis after meiosis. This proteolysis was specific for KCA-1 as GFP:calmodulin (CMD-1) showed no decrease in cytoplasmic fluorescence intensity in the +2 relative to the +1 embryo (Figures 5C and 5D). In worms depleted of the APC subunit, MAT-1, by RNAi, the +1 embryo exhibited a wild-type metaphase I packing of cytoplasmic mCherry:KCA-1 (Figure 5C). However, the fluorescence intensity dropped in the +2 and +3 embryos even though they were arrested at metaphase I. The small amount of KCA-1 remaining in +2 and +3 embryos of APC-depleted embryos was sequestered in structures that were never observed in wild-type (Figure 5C). In contrast, degradation of GFP:cyclin B1 was completely blocked by *mat-1(RNAi)* (Figures 5C and 5D). This result strongly suggests that KCA-1 is degraded late in meiosis and that a majority of KCA-1 is degraded in an APC-independent manner. The partial degradation of KCA-1 in APC-depleted embryos explains why partial centrosome maturation occurs in metaphase-arrested, APC-depleted embryos (Figures 5A and 5B). These results suggest that wild-type centrosome maturation may be initiated by KCA-1 degradation late in meiosis. Cowan and Hyman (2006) reported a delay in centrosome maturation in embryos depleted of cyclin E or CDK-2. Consistent with previous findings, we found that only 2/13 *cdk-2(RNAi)* embryos had a focus of GFP:TAC-1 associated with the male pronucleus in contrast with 9/11 wild-type embryos. However, no enrichment of KCA-1, UNC-116, or KLC-1 was observed around the male pronuclei of *cdk-2(RNAi)* embryos just as they were absent from the male pronuclei of wild-type embryos (Figures 2G, 2J, 2N, and 2Q). Thus, cyclin E/CDK-2 does not appear to promote sperm centrosome maturation by initiating degradation of KCA-1.

DISCUSSION

Because fertilization occurs during female meiosis and because sperm-derived centrioles form sperm asters equipped to capture the female pronucleus, all animals must actively prevent sperm asters from interfering with meiotic spindles until after extrusion of the second polar body. *C. elegans* uses at least two mechanisms to accomplish this: (1) the meiotic spindle and sperm are positioned at opposite ends of the zygote and (2) recruitment of pericentriolar proteins to the sperm centrioles is suppressed so that asters do not form until after extrusion of the second polar body. Kinesin-1 and its binding partner, KCA-1, are involved in both of these mechanisms.

Early in diakinesis, the prophase nucleus or germinal vesicle is centered within the oocyte. The germinal vesicle then migrates away from the end of the oocyte that is closest to the sperm in the spermatheca. This directed migration requires kinesin-1/KCA-1 (McNally et al., 2010). Fertilization then occurs at the end of the oocyte that first enters the spermatheca (Samuel et al., 2001). This system results in the rough placement of the meiotic spindle and sperm at opposite ends of the oval embryo long before establishment of embryonic polarity, which is induced by the sperm aster after completion of meiosis (Gönczy and Rose, 2005). During meiotic metaphase I and II, the spindle is maintained at the future anterior cortex by kinesin-1/KCA-1 (Yang et al., 2005), whereas during anaphase I and II the spindle is anchored at the cortex by cytoplasmic dynein (Ellefson and McNally, 2009; 2011). Positioning of the sperm DNA during female meiosis is more enigmatic. Kinesin-1/KCA-1 appears to transport the sperm DNA inward from the site of fertilization at the plasma membrane but the sperm DNA is maintained in the future posterior third of the embryo by an unknown mechanism. This migration of the sperm DNA is counterintuitive because it places the sperm DNA closer to the meiotic spindle. In fact, the average minimum distance between sperm DNA and meiotic spindle is not significantly different ($p = .16$, unpaired t test) between wild-type (27.8 ± 1.7 μm, $n = 24$) and *kca-1(RNAi)* (24.2 ± 1.6 μm, $n = 15$). Even though the meiotic spindle is further from the future anterior cortex in *kca-1(RNAi)* embryos, the sperm DNA is also closer to the future posterior cortex. Because cortical contact by the sperm aster initiates establishment of embryonic polarity in *C. elegans* (Gönczy and Rose, 2005), the inward transport of the sperm might be important in preventing premature polarity establishment. Two time-lapse studies of human fertilization reported that the male pronucleus always forms in the center of the zygote (Mio, 2006; Payne et al., 1997). This result indicates that the sperm DNA must be transported inward from the site of fertilization in human zygotes, which do not use the sperm as a cue for establishing embryonic polarity (Cooke et al., 2003). Depending on the sizes of the oocyte, spindle and sperm aster, centering the sperm while anchoring the spindle at the cortex might serve the general purpose of keeping the spindle and sperm apart.

Kinesin-1/KCA-1 is also essential for blocking recruitment of the maternal pericentriolar proteins, SPD-5 and γ-tubulin, to the sperm-derived centrioles. Unlike other kinesin-1/KCA-1-dependent processes like germinal vesicle positioning (Yang et al., 2003; McNally et al., 2010), meiotic spindle positioning (Yang et al., 2003; 2005), and sperm DNA positioning (this study), inhibition of pericentriolar protein recruitment to sperm centrioles does not require cytoplasmic microtubules and therefore cannot involve transport by kinesin on cytoplasmic microtubules. The requirement for the centriolar protein, SPD-2, in assembly of a shell of kinesin-1/KCA-1 around the sperm DNA and centrioles suggests a direct or indirect interaction between kinesin-1/KCA-1 and SPD-2. The shell of kinesin-1/KCA-1 might directly block diffusion of large complexes of pericentriolar material (PCM) from the cytoplasm to the centrioles or act as a scaffold for phosphatases that oppose PCM recruitment. Alternatively kinesin-1/KCA-1 might act more globally on the large cytoplasmic pool of SPD-2. Disruption of this pathway only resulted in spindle capture by the sperm aster in cases where the sperm aster and spindle ended up in close proximity.

The importance of sperm aster suppression in human zygotes is difficult to discern from the literature. The time between sperm-egg fusion and second polar body extrusion after in vitro fertilization is difficult to interpret from published studies (Mio, 2006) in part because of the long and heterogeneous time required for the sperm to traverse the zona pellucida. Intracytoplasmic injection of sperm eliminates these uncertainties and the second

polar body is extruded on average 2 hr after injection of human sperm into human oocytes (Mio, 2006; Payne et al., 1997). This would appear to be sufficient time for a sperm aster to form and interfere with anaphase II. The invasive methods required to unambiguously score sperm aster formation are not compatible with assisted reproduction in humans. However, when human sperm is injected into bovine oocytes, sperm aster formation is suppressed during anaphase II and does not occur until decondensation of both male and female pronuclei (Nakamura et al., 2001). It is likely that the use of advanced polarization microscopy (Kilani et al., 2011) will allow noninvasive analysis of sperm aster formation in human zygotes.

The finding that KCA-1 is degraded during meiosis suggests that normal centrosome maturation after meiosis is initiated by regulated proteolysis of KCA-1. Numerous proteins are degraded by different ubiquitin ligases in a highly ordered temporal sequence during or shortly after meiosis in *C. elegans*. For example, CAV-1 is degraded during meiosis in an endocytosis-dependent manner (Sato et al., 2006). MEI-1 is degraded at the exit from meiosis by a CUL-3-dependent mechanism (Pintard et al., 2003). OMA-1 is degraded after the first mitotic cleavage (Nishi and Lin, 2005). Although each of these proteins is degraded at a different time by a different mechanism, degradation of CAV-1 (Sato et al., 2006), MEI-1 and OMA-1 (Pellettieri et al., 2003) are also blocked in embryos arrested in meiotic metaphase I by depletion of anaphase promoting complex subunits (Pellettieri et al., 2003). The surprising finding that KCA-1 is degraded and that centrosomes mature in metaphase-arrested, APC-depleted embryos indicates that multiple, synchronized but independent clocks control the transition from oocyte to embryo.

EXPERIMENTAL PROCEDURES

C. elegans Strains

In this study, wild-type was N2 Bristol. The following transgenic strains were used: GFP:γ-tubulin/OD44: [*pie-1:GFP:tbg-1* + *unc-119(+)*] (provided by Karen Oegema, UCSD), DE90: oxIs318 [*spe-11::mCherry::histone* + *unc-119(+)*] II, ruIs32 [*pie-1::GFP::histone H2B* + *unc-119(+)*] III, ddIs6 [*tbg-1::GFP* + *unc-119(+)*], dnIs17 [*pie-1::GFP::PLC-PH domain* + *unc-119(+)*] (Johnston et al., 2010), GFP:TAC-1/JA1334 (Le Bot et al., 2003), GFP:tubulin + mCherry:histone/FM125 (Ellefson and McNally, 2011), mat-2(ts) + GFP: tubulin/FM157 (Ellefson and McNally, 2011), HR399: *unc-36(e251), unc-116(f130)* III, FM106: Is[*pie-1:mCherry:KLC-1* + *unc-119(+)*], FM105: Is[*pie-1:mCherry:KCA-1* + *unc-119(+)*], WH280/GFP:calmodulin (Batchelder et al., 2007), FM145: *unc-36(e251), unc-116(f130)* III, pwIs23 [*GFP:vit-2*], YP170 /RT368: *unc-119(ed3)* III; pwIs98 [*YP170::tdimer2* + *unc-119(+)*] (provided by Barth Grant, Rutgers University).

RNA Interference

All of the RNA interference (RNAi) experiments performed were carried out by feeding bacteria (HT115) induced to express double-stranded RNA corresponding to each gene as described by Timmons et al. (2001). L4 hermaphrodites were transferred to RNAi plates and allowed to feed on the RNAi bacterial lawn for 24–36 hr. All bacterial strains have been described previously (McNally et al., 2010; Ellefson and McNally, 2011). RNAi of *unc-116* was carried out on strain CB91 [*rol-1(e91)*II] as N2 was resistant to RNAi by feeding for this gene.

Live Imaging

Briefly, adult hermaphrodites were anesthetized with tricaine/tetramisole and immobilized between a coverslip and agarose pad on a slide as previously described (Ellefson and McNally, 2011). Time-lapse imaging was done on an Olympus IX71 inverted microscope equipped with a 60× PlanApo NA 1.42 objective and a Hamamatsu Orca R2 deep cooled C10600-10B digital mono CCD camera. Excitation light was shuttered with a Sutter shutter controlled by a Sutter Lambda 10-3 controller and MetaMorph Imaging software through a Sutter excitation filter wheel. For DE90 (Figure S1) and FM125 (Figure 4), pairs of single focal plane red and green fluorescence images were captured at 10 s intervals. Manual focus control was used to switch between the spindle and sperm. For imaging mCherry:KCA-1 and mCherry:KLC-1 (Figure 2), transgenes were first desilenced with *mut-16(RNAi)*, worms were mounted as above and single time point, single focal plane images were acquired with a Perkin Elmer Ultraview spinning disk confocal microscope.

Antibodies

Anti-SPD-5 and anti-SPD-2 rabbit antibodies were provided by Karen Oegema (UCSD). Rabbit antisera for UNC-116, KCA-1, and KLC-1 were described previously (McNally et al., 2010). For this study, *Escherichia coli* expressed UNC-116, KLC-1, and KCA-1 were immobilized on Affigel 15 beads (Biorad) and antibodies were bound, washed and eluted with 200 mM glycine pH 2.4 then neutralized with Tris 8.0 before use. Anti-γ-tubulin was from Sigma (LL17) and anti-α tubulin was from Sigma (DM1A).

Immunofluorescence

Meiotic embryos were dissected from adult hermaphrodites, freeze cracked and fixed with cold methanol as previously described (Ellefson and McNally, 2011). Complete Z stacks were captured for each meiotic embryo with an Olympus DSU spinning disk confocal using a 60× Plan Apo 1.42 objective and a Hamamatsu Orca R2 CCD. Maximum intensity projections were generated to include the meiotic spindle, polar bodies and sperm DNA/centrosomes.

Estimate of the Metaphase Arrest Time in *mat-2(ts)* Embryos

In living *mat-2(ts)*; GFP:histone worms shifted to nonpermissive temperature, chromosomes are decondensed in the embryos starting at the +5 position from the spermatheca. Since oocytes ovulate on average every 23 min (McCarter et al., 1999), the embryo in the +4 position has been arrested between 69 and 92 min. Because embryos must be dissected from the worm for fixed immunofluorescence, we used the condensation state of the chromosomes to restrict the analysis in Figure 6 to embryos arrested at metaphase I between 0 and 92 min.

SUPPLEMENTAL INFORMATION

Supplemental Information includes three figures and one table and can be found with this article online at doi:10.1016/j.devcel.2012.01.010.

ACKNOWLEDGMENTS

We thank Karen Oegema for antibodies, Bruce Bowerman, Kevin O'Connel, and The Caenorhabditis Genetics Cener for strains, and Yuji Kohara for cDNA clones. This work was supported by grant 1R01GM-079421 from the National Institute of General Medical Science to F.J.M.

Received: August 17, 2010
Revised: December 3, 2011
Accepted: January 12, 2012
Published online: March 29, 2012

REFERENCES

Albertson, D.G., and Thomson, J.N. (1993). Segregation of holocentric chromosomes at meiosis in the nematode, Caenorhabditis elegans. Chromosome Res. *1*, 15–26.

Batchelder, E.L., Thomas-Virnig, C.L., Hardin, J.D., and White, J.G. (2007). Cytokinesis is not controlled by calmodulin or myosin light chain kinase in the Caenorhabditis elegans early embryo. FEBS Lett. *581*, 4337–4341.

Cooke, S., Tyler, J.P., and Driscoll, G.L. (2003). Meiotic spindle location and identification and its effect on embryonic cleavage plane and early development. Hum. Reprod. *18*, 2397–2405.

Cowan, C.R., and Hyman, A.A. (2006). Cyclin E-Cdk2 temporally regulates centrosome assembly and establishment of polarity in Caenorhabditis elegans embryos. Nat. Cell Biol. *8*, 1441–1447.

Ellefson, M.L., and McNally, F.J. (2009). Kinesin-1 and cytoplasmic dynein act sequentially to move the meiotic spindle to the oocyte cortex in *Caenorhabditis elegans*. Mol. Biol. Cell *20*, 2722–2730.

Ellefson, M.L., and McNally, F.J. (2011). CDK-1 inhibits meiotic spindle shortening and dynein-dependent spindle rotation in *C. elegans*. J. Cell Biol. *193*, 1229–1244.

Gönczy, P., and Rose, L.S. (2005). Asymmetric cell division and axis formation in the embryo. In WormBook, The C. elegans Research Community, ed., 10.1895/wormbook.1.30.1, http://www.wormbook.org.

Gould, M.C., and Stephano, J.L. (1999). MAP kinase, meiosis, and sperm centrosome suppression in *Urechis caupo*. Dev. Biol. *216*, 348–358.

Hamill, D.R., Severson, A.F., Carter, J.C., and Bowerman, B. (2002). Centrosome maturation and mitotic spindle assembly in *C. elegans* require SPD-5, a protein with multiple coiled-coil domains. Dev. Cell *3*, 673–684.

Harris, P., Osborn, M., and Weber, K. (1980). Distribution of tubulin-containing structures in the egg of the sea urchin *Strongylocentrotus purpuratus* from fertilization through first cleavage. J. Cell Biol. *84*, 668–679.

Johnston, W.L., Krizus, A., and Dennis, J.W. (2010). Eggshell chitin and chitin-interacting proteins prevent polyspermy in *C. elegans*. Curr. Biol. *20*, 1932–1937.

Kemp, C.A., Kopish, K.R., Zipperlen, P., Ahringer, J., and O'Connell, K.F. (2004). Centrosome maturation and duplication in *C. elegans* require the coiled-coil protein SPD-2. Dev. Cell *6*, 511–523.

Kilani, S., Cooke, S., Tilia, L., and Chapman, M. (2011). Does meiotic spindle normality predict improved blastocyst development, implantation and live birth rates? Fertil. Steril. *96*, 389–393.

Kim, D.Y., and Roy, R. (2006). Cell cycle regulators control centrosome elimination during oogenesis in *Caenorhabditis elegans*. J. Cell Biol. *174*, 751–757.

Le Bot, N., Tsai, M.C., Andrews, R.K., and Ahringer, J.; TAC-1. (2003). TAC-1, a regulator of microtubule length in the C. elegans embryo. Curr. Biol. *13*, 1499–1505.

Lee, M.H., Ohmachi, M., Arur, S., Nayak, S., Francis, R., Church, D., Lambie, E., and Schedl, T. (2007). Multiple functions and dynamic activation of MPK-1 extracellular signal-regulated kinase signaling in *Caenorhabditis elegans* germline development. Genetics *177*, 2039–2062.

Leidel, S., and Gönczy, P. (2005). Centrosome duplication and nematodes: recent insights from an old relationship. Dev. Cell *9*, 317–325.

Li, S., Armstrong, C.M., Bertin, N., Ge, H., Milstein, S., Boxem, M., Vidalain, P.O., Han, J.D., Chesneau, A., Hao, T., et al. (2004). A map of the interactome network of the metazoan *C. elegans*. Science *303*, 540–543.

McCarter, J., Bartlett, B., Dang, T., and Schedl, T. (1999). On the control of oocyte meiotic maturation and ovulation in *Caenorhabditis elegans*. Dev. Biol. *205*, 111–128.

McNally, K.L., and McNally, F.J. (2005). Fertilization initiates the transition from anaphase I to metaphase II during female meiosis in *C. elegans*. Dev. Biol. *282*, 218–230.

McNally, K.L., Martin, J.L., Ellefson, M., and McNally, F.J. (2010). Kinesin-dependent transport results in polarized migration of the nucleus in oocytes and inward movement of yolk granules in meiotic embryos. Dev. Biol. *339*, 126–140.

Mio, Y. (2006). Morphological analysis of human embryonic development using time-lapse cinematography. J. Mamm. Ova Res. *23*, 27–36.

Nakamura, S., Terada, Y., Horiuchi, T., Emuta, C., Murakami, T., Yaegashi, N., and Okamura, K. (2001). Human sperm aster formation and pronuclear decondensation in bovine eggs following intracytoplasmic sperm injection using a Piezo-driven pipette: a novel assay for human sperm centrosomal function. Biol. Reprod. *65*, 1359–1363.

Navara, C.S., First, N.L., and Schatten, G. (1994). Microtubule organization in the cow during fertilization, polyspermy, parthenogenesis, and nuclear transfer: the role of the sperm aster. Dev. Biol. *162*, 29–40.

Nishi, Y., and Lin, R. (2005). DYRK2 and GSK-3 phosphorylate and promote the timely degradation of OMA-1, a key regulator of the oocyte-to-embryo transition in *C. elegans*. Dev. Biol. *288*, 139–149.

Oegema, K., and Hyman, A.A. (2006). Cell division. In WormBook, The *C. elegans* Research Community, ed. WormBook, 10.1895/wormbook.1.72.1.

O'Rourke, S.M., Carter, C., Carter, L., Christensen, S.N., Jones, M.P., Nash, B., Price, M.H., Turnbull, D.W., Garner, A.R., Hamill, D.R., et al. (2011). A survey of new temperature-sensitive, embryonic-lethal mutations in *C. elegans*: 24 alleles of thirteen genes. PLoS ONE *6*, e16644.

Parvin, J.D. (2009). The BRCA1-dependent ubiquitin ligase, γ-tubulin, and centrosomes. Environ. Mol. Mutagen. *50*, 649–653.

Payne, D., Flaherty, S.P., Barry, M.F., and Matthews, C.D. (1997). Preliminary observations on polar body extrusion and pronuclear formation in human oocytes using time-lapse video cinematography. Hum. Reprod. *12*, 532–541.

Pelletier, L., Ozlü, N., Hannak, E., Cowan, C., Habermann, B., Ruer, M., Müller-Reichert, T., and Hyman, A.A. (2004). The *Caenorhabditis elegans* centrosomal protein SPD-2 is required for both pericentriolar material recruitment and centriole duplication. Curr. Biol. *14*, 863–873.

Pelletier, L., O'Toole, E., Schwager, A., Hyman, A.A., and Müller-Reichert, T. (2006). Centriole assembly in *Caenorhabditis elegans*. Nature *444*, 619–623.

Pellettieri, J., Reinke, V., Kim, S.K., and Seydoux, G. (2003). Coordinate activation of maternal protein degradation during the egg-to-embryo transition in *C. elegans*. Dev. Cell *5*, 451–462.

Pintard, L., Willis, J.H., Willems, A., Johnson, J.L., Srayko, M., Kurz, T., Glaser, S., Mains, P.E., Tyers, M., Bowerman, B., and Peter, M. (2003). The BTB protein MEL-26 is a substrate-specific adaptor of the CUL-3 ubiquitin-ligase. Nature *425*, 311–316.

Rappleye, C.A., Tagawa, A., Lyczak, R., Bowerman, B., and Aroian, R.V. (2002). The anaphase-promoting complex and separin are required for embryonic anterior-posterior axis formation. Dev. Cell *2*, 195–206.

Sakamoto, R., Byrd, D.T., Brown, H.M., Hisamoto, N., Matsumoto, K., and Jin, Y. (2005). The *Caenorhabditis elegans* UNC-14 RUN domain protein binds to the kinesin-1 and UNC-16 complex and regulates synaptic vesicle localization. Mol. Biol. Cell *16*, 483–496.

Samuel, A.D., Murthy, V.N., and Hengartner, M.O. (2001). Calcium dynamics during fertilization in *C. elegans*. BMC Dev. Biol. *1*, 8.

Sato, K., Sato, M., Audhya, A., Oegema, K., Schweinsberg, P., and Grant, B.D. (2006). Dynamic regulation of caveolin-1 trafficking in the germ line and embryo of *Caenorhabditis elegans*. Mol. Biol. Cell *17*, 3085–3094.

Schott, S., Coustham, V., Simonet, T., Bedet, C., and Palladino, F. (2006). Unique and redundant functions of *C. elegans* HP1 proteins in post-embryonic development. Dev. Biol. *298*, 176–187.

Song, M.H., Aravind, L., Müller-Reichert, T., and O'Connell, K.F. (2008). The conserved protein SZY-20 opposes the Plk4-related kinase ZYG-1 to limit centrosome size. Dev. Cell *15*, 901–912.

Stearns, T., and Kirschner, M. (1994). In vitro reconstitution of centrosome assembly and function: the central role of γ-tubulin. Cell *76*, 623–637.

Stephano, J.L., and Gould, M.C. (2000). MAP kinase, a universal suppressor of sperm centrosomes during meiosis? Dev. Biol. *222*, 420–428.

Timmons, L., Court, D.L., and Fire, A. (2001). Ingestion of bacterially expressed dsRNAs can produce specific and potent genetic interference in *Caenorhabditis elegans*. Gene *263*, 103–112.

Toda, H., Mochizuki, H., Flores, R., 3rd, Josowitz, R., Krasieva, T.B., Lamorte, V.J., Suzuki, E., Gindhart, J.G., Furukubo-Tokunaga, K., and Tomoda, T. (2008). UNC-51/ATG1 kinase regulates axonal transport by mediating motor-cargo assembly. Genes Dev. *22*, 3292–3307.

Ward, S., Argon, Y., and Nelson, G.A. (1981). Sperm morphogenesis in wild-type and fertilization-defective mutants of *Caenorhabditis elegans*. J. Cell Biol. *91*, 26–44.

Tsuboi, D., Hikita, T., Qadota, H., Amano, M., and Kaibuchi, K. (2005). Regulatory machinery of UNC-33 Ce-CRMP localization in neurites during neuronal development in *Caenorhabditis elegans*. J. Neurochem. *95*, 1629–1641.

Wu, X., and Palazzo, R.E. (1999). Differential regulation of maternal vs. paternal centrosomes. Proc. Natl. Acad. Sci. USA *96*, 1397–1402.

Yang, H.Y., McNally, K., and McNally, F.J. (2003). MEI-1/katanin is required for translocation of the meiosis I spindle to the oocyte cortex in C elegans. Dev. Biol. *260*, 245–259.

Yang, H.Y., Mains, P.E., and McNally, F.J. (2005). Kinesin-1 mediates translocation of the meiotic spindle to the oocyte cortex through KCA-1, a novel cargo adapter. J. Cell Biol. *169*, 447–457.

Zhou, K., Rolls, M.M., Hall, D.H., Malone, C.J., and Hanna-Rose, W. (2009). A ZYG-12-dynein interaction at the nuclear envelope defines cytoskeletal architecture in the *C. elegans* gonad. J. Cell Biol. *186*, 229–241.